



Published in final edited form as:

J Mol Biol. 2013 May 27; 425(10): . doi:10.1016/j.jmb.2013.02.016.

Ultrasensitivity of an adaptive bacterial motor

Junhua Yuan and Howard C. Berg

Department of Molecular and Cellular Biology, Harvard University, Cambridge, MA 02138

Abstract

The flagellar motor of *Escherichia coli* has been shown to adapt to changes in the steady-state level of the chemotaxis response regulator, CheY-P, by adjusting the number of molecules to which CheY-P binds, FliM. Previous measurements of motor ultrasensitivity have been made on cells containing different amounts of CheY-P, and thus different amounts of FliM. Here, we designed an experiment to measure the sensitivity of motors containing fixed amounts of FliM, finding Hill coefficients about twice as large as those observed before. This ultrasensitivity provides further insights into the motor switching mechanism and plays important roles in chemotaxis signal amplification and coordination of multiple motors. The Hill coefficients observed here appear to be the highest known for allosteric protein complexes, either biological or synthetic. Extreme motor ultrasensitivity broadens our understanding of mechanisms of allostery, and serves as an inspiration for future design of synthetic protein switches.

Keywords

cooperativity; allostery; molecular motor; switch; chemotaxis

Introduction

Cells of *Escherichia coli* are propelled by several helical filaments, each driven at its base by a reversible rotary motor. When all the motors of a cell rotate counterclockwise (CCW), the filaments form a bundle and the cell swims smoothly. When one or more motors rotate clockwise (CW), their filaments come out of the bundle and the cell changes course¹. The cell performs chemotaxis in a biased random walk², by modulating the direction of flagellar rotation^{3;4}. Chemoreceptors in the cell membrane sense changes in the concentrations of environmental chemical attractants or repellents, regulating the activity of a kinase that phosphorylates a response regulator, CheY^{5;6}. CheY-P binds to a component of the switch complex at the base of the flagellar motor, FliM, increasing the fraction of time that the motor spins CW (raising the CW bias)^{7;8}.

The motor is very sensitive to the concentration of CheY-P, [CheY-P]. This sensitivity is commonly characterized by a Hill coefficient, n , obtained by fitting the motor CW bias vs. [CheY-P] relationship with the Hill function $1/(1+(K_{1/2}/[\text{CheY-P}])^n)$, where $K_{1/2}$ is the concentration at which CW bias is 0.5. Measurements in bacterial populations reported values of the Hill coefficient ranging from 3.5 to 5.5^{9;10}. Measurements with single cells removed complications due to averaging over cell populations and reported a value of the Hill coefficient of 10.3¹¹. Recently, the flagellar motor was found to partially adapt to variations in the concentration of CheY-P by changing the number of FliM subunits in its switch complex¹². Therefore, the measurements made with single cells were actually

measurements of cells that had adapted to different levels of CheY-P, representing an average over motors with different complements of FliM. To learn the actual response of the motor, the input-output relationship should be measured for motors with a fixed number of FliM subunits.

Results

Here, we designed an experiment that used a bead assay to accomplish this task, Fig. 1. Panel **a** shows the CW bias and panel **b** the intracellular CheY-P concentration, [CheY-P], both as a function of time. The bias was measured by the bead assay, while the CheY-P concentration was inferred from the bias measurement. We used a *cheR cheB* strain, so that when the attractant was added, the intracellular CheY-P concentration changed from C_1 to C_2 and remained constant^{12; 13}. In contrast, the CW bias changed from B_1 to B_2 and slowly adapted to B_3 ¹². When the attractant was removed, the intracellular CheY-P concentration changed from C_2 back to the pre-stimulus value C_1 ¹³, while the CW bias changed from B_3 to B_4 and slowly adapted back to the pre-stimulus value B_1 . Since the motor was adapted before attractant addition and removal, C_1 and C_2 can be extracted from B_1 and B_3 using the relationship measured by Cluzel *et al.*¹¹, which is a relationship for adapted motors. At the instant of attractant addition, the motor has yet to adapt, so (C_1, B_1) and (C_2, B_2) correspond to the input-output of a motor with a fixed number of FliM subunits, a motor with an adapted CW bias B_1 . Similarly, at the instant of attractant removal, (C_2, B_3) and (C_1, B_4) correspond to the input-output of a motor with a fixed number of FliM subunits, a motor with an adapted CW bias B_3 . We performed single-motor measurements on a population of cells with various pre-stimulus biases, B_1 , and various responses to attractant addition and removal, B_2, B_3 , and B_4 . Since there is a one-to-one relationship between the number of FliM subunits in a motor and the adapted CW bias¹², we can group the data points according to the adapted CW bias (B_1 and B_3) and obtain a full input-output relationship.

An example of the CW bias as a function of time using the bead assay is shown in Fig. 2, which shows the averaged responses of nine motors on different cells to stepwise addition and removal of 0.5 mM MeAsp, added near 70 s and removed near 400 s.

Two measured input-output relationships are shown in Fig. 3, corresponding to motors with an adapted CW bias 0.8 ± 0.1 (panel **a**) and 0.5 ± 0.1 (panel **b**). In each figure, the red curve shows the Hill function obtained by Cluzel *et al.*¹¹ with Hill coefficient 10.3. Data points below the red curve were obtained from attractant addition, while data points above the red curve were obtained from attractant removal. Data points on the red curve, shown with red symbols, were the initial values for the adapted motors. The fits to a Hill function are shown by the blue curves, yielding a Hill coefficient 16.5 ± 1.8 and dissociation constant $3.28 \pm 0.02 \mu\text{M}$ for motors with an adapted bias of 0.8 (panel **a**), and a Hill coefficient 20.7 ± 1.6 and dissociation constant of $3.12 \pm 0.01 \mu\text{M}$ for motors with an adapted bias of 0.5 (panel **b**). The sensitivities (Hill coefficients) are about twice that of the previous measurement made with single cells. In the Monod-Wyman-Changeux (MWC) model of the motor^{10; 14}, the sensitivity (Hill coefficients) increases with the number of FliM units N , while $K_{1/2}$ decreases with N ¹⁵. Our results thus suggest that the number of FliM units in motors with an adapted bias of 0.5 is larger than that in motor with an adapted bias of 0.8, consistent with the previous study of motor adaptation¹².

In the previous study¹², we used the curve measured by Cluzel *et al.* as the relationship for pre-adapted motors with a specific number of FliM units, and based on this, we constructed a new relationship for the motor with a larger number of FliM units. According to the present study, the curve for the pre-adapted motor with a specific number of FliM units is actually about a factor of two steeper than what Cluzel *et al.* measured.

In the conformational spread model of the motor switch¹⁶, this ultrasensitivity (a sensitivity larger than 16) can be explained by the large number of protomers ($N \sim 34$), a high bi-stability of the protomer structure (with the energy difference between CW and CCW states of each protomer, E_a , larger than 1 kT), and a strong coupling between the protomers (with the coupling energy between neighboring protomers, E_j , larger than 4 kT); see Supplementary Materials. The ultrasensitivity observed here is even more impressive considering the fact that the motor keeps remodeling itself by varying the number of FliM units. How does the motor switch maintain such variability while exhibiting a high stability with strong coupling between protomers? The FliG proteins, another component of the motor switch, might confer this high stability while turn-over of the FliM proteins provides the variability. This is in line with a recent discovery showing non-exchange of FliG proteins in the motor for hours¹⁷, while turn-over of FliM proteins happens in tens of seconds¹⁸.

The conformational spread model predicts that a motor exhibiting a sensitivity of 16 would show a CheY-P binding cooperativity of about 9 (see Supplemental Materials). The highest binding cooperativity reported thus far is less than 2⁸. A more careful measurement of the CheY-P binding cooperativity is needed. If higher binding cooperativities are not found, one might have to consider non-equilibrium models for switching, such as the one proposed by Tu¹⁹.

Discussion

Sensitivity of the motor contributes to signal amplification in chemotaxis. The ultrasensitivity measured in this study shows that it plays a more important role than previously thought. Moreover, ultrasensitivity of the motor is critical for coordination of multiple motors in a cell by fluctuations or bursts in the intracellular concentration of CheY-P. The rotational bias between adjacent motors was observed to be correlated over a time scale of about 10 s²⁰. This was attributed to slow fluctuations in the steady state [CheY-P] due to fluctuations in the receptor adaptation kinetics, and was found to enhance the sensitivity of bacterium to very shallow gradients of attractants²¹. This steady-state [CheY-P] fluctuation remains to be shown directly. Ultrasensitivity of the motor makes the bias correlation possible even with [CheY-P] fluctuations of small amplitude. Recently, coordinated switching between adjacent motors was documented on a subsecond timescale, and was postulated to arise from a burst of CheY-P propagating from the cell pole that drives the motor bias from 0% to 100% CW or vice versa²². Such CheY-P bursts also remain to be shown directly. High motor ultrasensitivity alleviates the requirement of large bursts. Therefore, previous studies of the motor bias correlation^{20; 21; 22} and previous proposals for the motor coordination mechanism²² should be revisited using our new values for motor sensitivity.

The ultrasensitivity (high switching cooperativity) observed here (Hill coefficient $n \sim 21$) is easily the highest found among allosteric protein complexes, e.g., hemoglobin ($n \sim 3$)²³, aspartate carbamoyltransferase ($n < 3$)²⁴, cytochrome P450 ($n < 4$)²⁵, the oligomeric chaperon GroEL ($n \sim 3$)²⁶, ion channels ($n \sim 3$)²⁷, and synthetic protein switches ($n \sim 4$)²⁸. We expect this ultrasensitivity will provide further insights into mechanisms of allostery and inspire future design of synthetic protein switches.

Materials and Methods

Strain JY35 [*cheR cheB fliC*] is a derivative of *E. coli* K12 strain RP437²⁹. The plasmid pKAF131 carrying the sticky *fliC* allele under control of the native *fliC* promoter³⁰ was transformed into JY35, yielding the strain used for this study. The bead assay was described

previously^{12,31}. Briefly, cells were grown at 33 °C in T-broth to an OD₆₀₀ between 0.45 and 0.50, washed twice with motility buffer (10 mM potassium phosphate, 0.1 mM EDTA, 1 μM methionine, 10 mM lactic acid, pH 7.0), sheared to truncate flagella, and concentrated by a factor of 2. The sheared cells were immobilized on a glass coverslip coated with poly-L-lysine (0.01%, P4707, Sigma, St. Louis, MO) and 1.0-μm-diameter polystyrene latex beads (2.69%, 07310, Polysciences, Warrington, PA) were attached to the truncated flagella. The coverslip was installed as the top window of a flow chamber³², and a constant flow of buffer (400 μl/min) was maintained by a syringe pump (Pump-22, Harvard Apparatus, Holliston, MA). The attractant used in this study was 0.5 mM γ -methyl-D,L-aspartate (MeAsp) in motility buffer. Rotation of the bead was monitored with a laser dark-field setup described previously³³. For each experiment, the bead was monitored for ~70 s in motility buffer, for ~330 s in the attractant solution, and again for about ~200 s in motility buffer. Data were analyzed using custom scripts in Matlab, and curves were fit with the nonlinear least square method in Matlab.

Supplementary Material

Refer to Web version on PubMed Central for supplementary material.

Acknowledgments

We thank Richard Branch for helpful comments. This work was supported by National Institutes of Health Grant AI016478.

References

1. Turner L, Ryu W, Berg HC. Real-time imaging of fluorescent flagellar filaments. *J Bacteriol.* 2000; 182:2793–2801. [PubMed: 10781548]
2. Berg HC, Brown DA. Chemotaxis in *Escherichia coli* analysed by three-dimensional tracking. *Nature.* 1972; 239:500–504. [PubMed: 4563019]
3. Berg HC, Anderson RA. Bacteria swim by rotating their flagellar filaments. *Nature.* 1973; 245:380–384. [PubMed: 4593496]
4. Larsen SH, Reader RW, Kort EN, Tso W, Adler J. Change in direction of flagellar rotation is the basis of the chemotactic response in *Escherichia coli*. *Nature.* 1974; 249:74–77. [PubMed: 4598031]
5. Hazelbauer GL, Falke JJ, Parkinson JS. Bacterial chemoreceptors: high performance signaling in networked arrays. *Trends Biochem Sci.* 2008; 33:9–19. [PubMed: 18165013]
6. Sourjik V. Receptor clustering and signal processing in *E. coli* chemotaxis. *Trends Microbiol.* 2004; 12:569–576. [PubMed: 15539117]
7. Welch M, Oosawa K, Aizawa S, Eisenbach M. Phosphorylation-dependent binding of a signal molecule to the flagellar switch of bacteria. *Proc Natl Acad Sci USA.* 1993; 90:8787–8791. [PubMed: 8415608]
8. Sourjik V, Berg HC. Binding of the *Escherichia coli* response regulator CheY to its target measured in vivo by fluorescence resonance energy transfer. *Proc Natl Acad Sci USA.* 2002; 99:12669–12674. [PubMed: 12232047]
9. Scharf BE, Fahrner KA, Turner L, Berg HC. Control of direction of flagellar rotation in bacterial chemotaxis. *Proc Natl Acad Sci USA.* 1998; 95:201–206. [PubMed: 9419353]
10. Alon U, Camarena L, Surette MG, Aguera y Arcas B, Liu Y, Leibler S, Stock JB. Response regulator output in bacterial chemotaxis. *EMBO J.* 1998; 17:4238–4248. [PubMed: 9687492]
11. Cluzel P, Surette M, Leibler S. An ultrasensitive bacterial motor revealed by monitoring signaling proteins in single cells. *Science.* 2000; 287:1652–1655. [PubMed: 10698740]
12. Yuan J, Branch RW, Hosu BG, Berg HC. Adaptation at the output of the chemotaxis signalling pathway. *Nature.* 2012; 484:233–236. [PubMed: 22498629]
13. Sourjik V, Berg HC. Receptor sensitivity in bacterial chemotaxis. *Proc Natl Acad Sci USA.* 2002; 99:123–127. [PubMed: 11742065]

14. Monod J, Wyman J, Changeux JP. On the nature of allosteric transitions: a plausible model. *J Mol Biol.* 1965; 12:88–118. [PubMed: 14343300]
15. Sourjik V, Berg HC. Functional interactions between receptors in bacterial chemotaxis. *Nature.* 2004; 428:437–441. [PubMed: 15042093]
16. Duke TAJ, Le Novere N, Bray D. Conformational spread in a ring of proteins: a stochastic approach to allostery. *J Mol Biol.* 2001; 308:541–553. [PubMed: 11327786]
17. Fukuoka H, Inoue Y, Terasawa S, Takahashi H, Ishijima A. Exchange of rotor components in functioning bacterial flagellar motor. *Biochem Biophys Res Commun.* 2010; 394:130–135. [PubMed: 20184859]
18. Delalez NJ, Wadhams GH, Rosser G, Xue Q, Brown MT, Dobbie IM, Berry RM, Leake MC, Armitage JP. Signal-dependent turnover of the bacterial flagellar switch protein FlIM. *Proc Natl Acad Sci USA.* 2010; 107:11347–11351. [PubMed: 20498085]
19. Tu Y. The nonequilibrium mechanism for ultrasensitivity in a biological switch: Sensing by Maxwell's demons. *Proc Natl Acad Sci USA.* 2008; 105:11737–11741. [PubMed: 18687900]
20. Ishihara A, Segall JE, Block SM, Berg HC. Coordination of flagella on filamentous cells of *Escherichia coli*. *J Bacteriol.* 1983; 155:228–237. [PubMed: 6345503]
21. Sneddon MW, Pontius W, Emonet T. Stochastic coordination of multiple actuators reduces latency and improves chemotactic response in bacteria. *Proc Natl Acad Sci USA.* 2012; 109:805–810. [PubMed: 22203971]
22. Terasawa S, Fukuoka H, Inoue Y, Sagawa T, Takahashi H, Ishijima A. Coordinated reversal of flagellar motors on a single *Escherichia coli* cell. *Biophys J.* 2011; 100:2193–2200. [PubMed: 21539787]
23. Wyman J. Allosteric effects in Hemoglobin. *Cold Spring Harb Symp Quant Biol.* 1963; 28:483–489.
24. Eisensteini E, Markby DW, Schachman HK. Changes in stability and allosteric properties of aspartate transcarbamoylase resulting from amino acid substitutions in the zinc-binding domain of the regulatory chains. *Proc Natl Acad Sci USA.* 1989; 86:3094–3098. [PubMed: 2566165]
25. Ueng Y, Kuwabara T, Chun Y, Guengerich FP. Cooperativity in oxidations catalyzed by cytochrome P450 3A4. *Biochemistry.* 1997; 36:370–381. [PubMed: 9003190]
26. Gray TE, Fersht AR. Cooperativity in ATP hydrolysis by GroEL is increased by GroES. *FEBS Lett.* 1991; 292:254–258. [PubMed: 1683631]
27. Liman ER, Buck LB. A second subunit of the olfactory cyclic nucleotide-gated channel confers high sensitivity to cAMP. *Neuron.* 1994; 13:611–621. [PubMed: 7522482]
28. Dueber JE, Mirsky EA, Lim WA. Engineering synthetic signaling proteins with ultrasensitive input/output control. *Nature biotechnol.* 2007; 25:660–662. [PubMed: 17515908]
29. Parkinson JS. Complementation analysis and deletion mapping of *Escherichia coli* mutants defective in chemotaxis. *J Bacteriol.* 1978; 135:45–53. [PubMed: 353036]
30. Yuan J, Fahrner KA, Turner L, Berg HC. Asymmetry in the clockwise and counter-clockwise rotation of the bacterial flagellar motor. *Proc Natl Acad Sci USA.* 2010; 107:12846–12949. [PubMed: 20615986]
31. Yuan J, Berg HC. Resurrection of the flagellar motor near zero load. *Proc Natl Acad Sci USA.* 2008; 105:1182–1185. [PubMed: 18202173]
32. Berg HC, Block SM. A miniature flow cell designed for rapid exchange of media under high-power microscope objectives. *J Gen Microbiol.* 1984; 130:2915–2920. [PubMed: 6396378]
33. Yuan J, Fahrner KA, Berg HC. Switching of the bacterial flagellar motor near zero load. *J Mol Biol.* 2009; 390:394–400. [PubMed: 19467245]

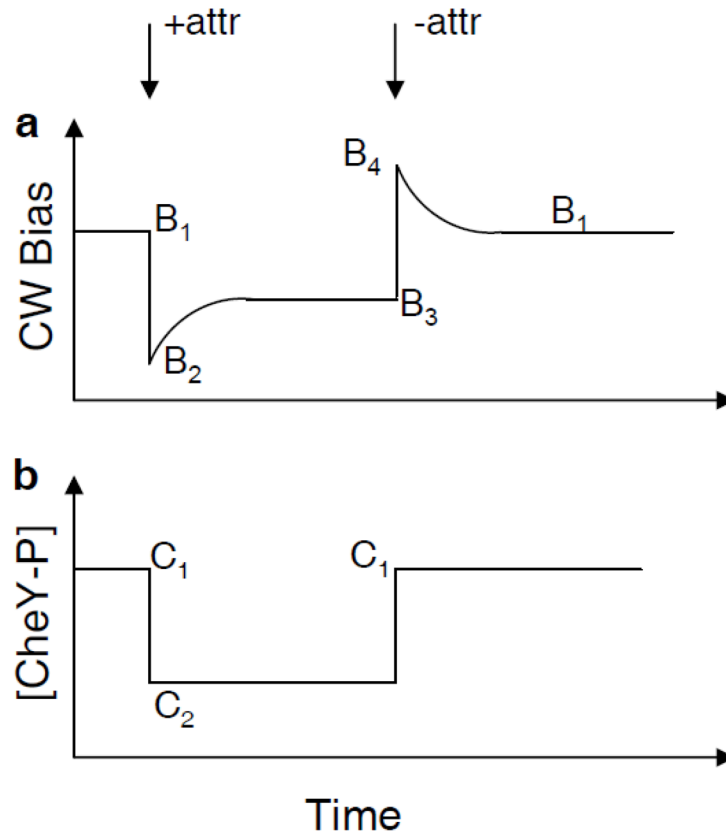


Fig. 1. Schematic of the response of *cheR cheB* cells to step addition and removal of a non-metabolizable attractant. **(a)** Motor CW bias as a function of time. **(b)** Intracellular CheY-P concentration as a function of time.

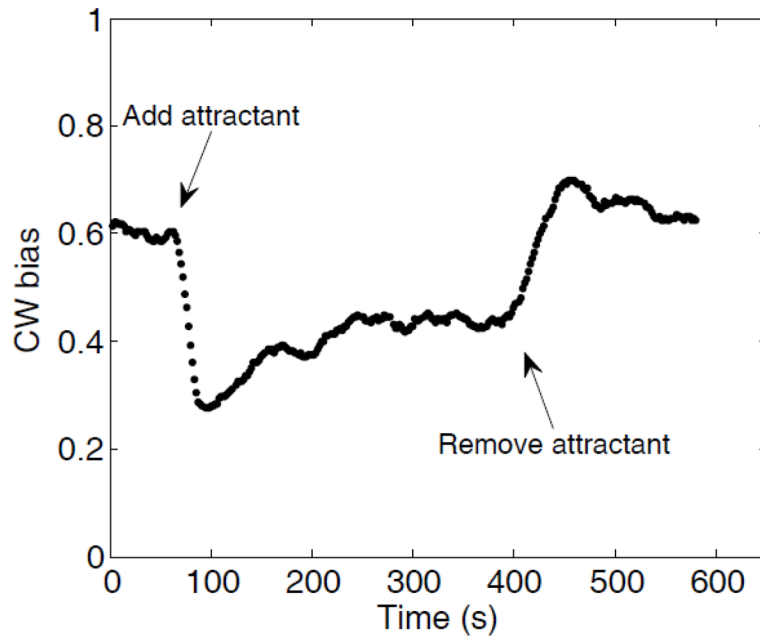


Fig. 2. Motor response of 9 *cheR cheB* cells to stepwise addition and removal of chemical attractant (0.5 mM MeAsp), monitored by the bead assay. The attractant was added and removed at the times indicated by the arrows.

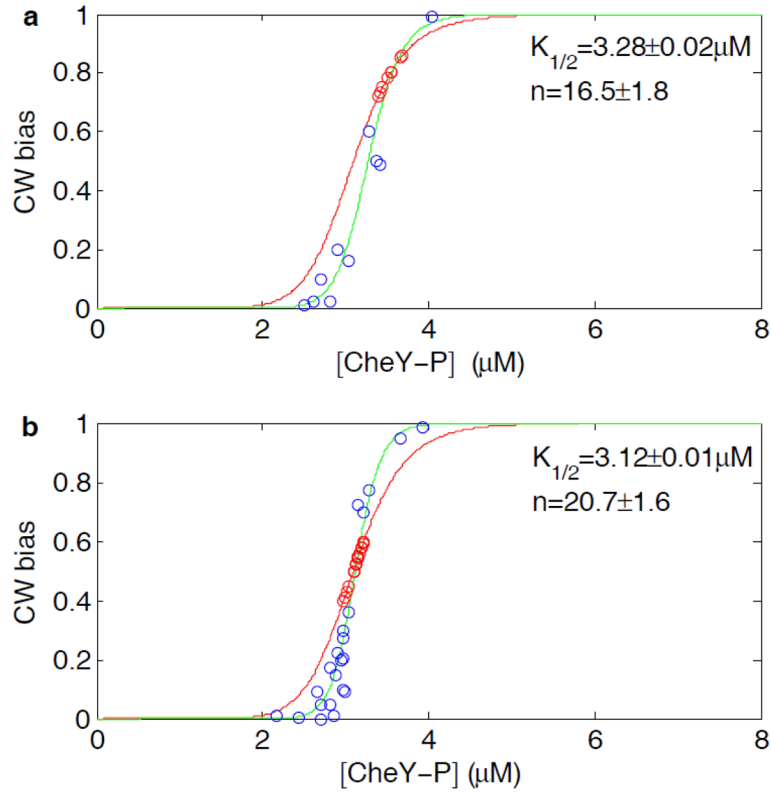


Fig. 3.

True input-output relationships of the motor. Blue and red circles are measurements in this study, and green curves are the corresponding fits with the Hill function. Red curves are the the Hill function fit to the data of Cluzel *et al.*¹¹. **(a)** Input-output relationship for motors with an adapted CW bias of 0.8 ± 0.1 . **(b)** Input-output relationship for motors with an adapted CW bias of 0.5 ± 0.1 .